Korean J. Chem. Eng., **18**(1), 120-126 (2001)

The Skeletal Isomerization of C_4-C_7 1-Olefins over Ferrierite and ZSM-5 Zeolite Catalysts

Wang-Gi Kim, Jong-Ho Kim, Byoung Joon Ahn* and Gon Seo†

Department of Chemical Technology and The Research Institute for Catalysis,
Chonnam National University, Gwangju 500-757, Korea
*Department of Chemistry Education, Chonbuk National University, Chonju 561-756, Korea
(*Received 16 August 2000 • accepted 4 December 2000*)

Abstract–The skeletal isomerization of C_4-C_7 1-olefins was studied on ferrierite (FER) and ZSM-5 (MFI) zeolites to elucidate the effect of the molecular distribution in zeolite pores on the selectivity for *iso*-olefin formation. Regardless of the difference in molecular length of 1-olefins, the FER zeolite showed high selectivity for *iso*-olefins, while the selectivity became slightly low at the skeletal isomerization of long olefin molecules. The drastic decrease in the selectivity of MFI zeolites by increasing the conversion is concurrently observed in the skeletal isomerization of C_4-C_7 1-olefins. The high selectivity of FER zeolites is explained by their sparse distributions of olefin molecules in pores, which induces a high preference for monomolecular skeletal isomerization.

Key words: C_4-C_7 1-Olefins, Skeletal Isomerization, Ferrierite, ZSM-5 Zeolite, Pore Shape

INTRODUCTION

Skeletal isomerization of *n*-butenes on various solid acid catalysts has been studied in regard to the selective production of *iso*-butene, which is a raw material of methyl *tert*-butyl ether (MTBE) used as an octane number booster [Choudhary et al., 1974; Butler and Nicolaides, 1993]. In addition to this economic objective, the fundamental cause of the exceptional selectivity of ferrierite (FER) for *iso*-butenes is also a particularly interesting research topic. The report on the phase-out of MTBE from gasoline due to its contamination of ground water reduces considerably the industrial interest in skeletal isomerization. However, investigations about the molecular behavior of butene molecules in FER zeolites resulting in exceptional selectivity are still being continued [Lee et al., 2000; Asensi and Martinez, 1999].

Since the skeletal isomerization of *n*-butene competes with its dimerization, selectivity for *iso*-butene is largely dependent on the suppression of dimerization which produces various hydrocarbons via cracking. Molecular dynamic simulation assumed that most butene molecules, either *n*-butenes or *iso*-butenes, were sparsely distributed on the FER zeolite at its cavities formed along 8-ring channels [Jousse et al., 1996, 1997; van Well et al., 1998; Seo et al., 1997]. Stabilization in cavity and high potential for transfer to other cavities reduce intermolecular collisions, the essential step of dimerization, resulting in the exceptional selectivity for monomolecular skeletal isomerization. Therefore, distant distribution of the adsorbed butene molecules is considered to be the fundamental cause suppressing the dimerization of butene molecules [Seo et al., 1998; Kim et al., 1999].

However, there is no meaningful restriction for the distribution of butene molecules in the ZSM-5 (MFI) zeolite [Seo et al., 1997]. Furthermore, the potential barrier for the transfer of butene molecules along the MFI zeolite pore is quite small compared to FER and clinoptilolite (CLI) zeolites. Thus, the low selectivity on the MFI zeolite is considered to be caused by the close distribution of butene molecules, preferring to form dimers which easily crack into various hydrocarbons on acid sites. The *in-situ* IR study illustrates that polymeric species are formed from adsorbed butene molecules on the MFI zeolite, while fast desorption of butene molecules from the FER zeolite assumes a monomolecular distribution [Seo et al., 2000]. Since molecularities of skeletal isomerization and dimerization are different as mono and bi, respectively, molecular distribution of butene molecules in the zeolite pore takes on the role of determining the selectivity for skeletal isomerization.

Since the cavity size of the FER zeolite is about 7 Å [van Well et al., 1998], distribution patterns of C_4-C_7 1-olefin molecules in pores may vary with their molecular lengths. Sparse distribution of olefin molecules, such as a molecule per cavity, can be expected when olefin molecules are sufficiently smaller than the cavity size. Large olefin molecules are not confined in the cavities; thus, their distribution patterns are not uniform as butene molecules. Nevertheless, the repulsion between adsorbed large olefin molecules as well as the restriction due to cavity structure of FER zeolite reduces the adsorbed amount of large olefin, bringing about also its sparse distribution.

On the other hand, low selectivities for the skeletal isomerization of C_4-C_7 1-olefins are consistently anticipated on the MFI zeolite, regardless of their molecular lengths. The sufficient cross-sectional area of an MFI zeolite pore for linear olefin molecules to diffuse in does not impose any meaningful constraint on the distribution of olefin molecules. High preference for close distribution, therefore, accelerates dimerization producing various hydrocarbons via cracking.

This work deals with the skeletal isomerization of C_4-C_7 1-olefins on FER and MFI zeolites to elucidate effects of the molecular length and pore shape on the reaction preference of olefins. Since large olefins have high cracking probabilities without forming di-

†To whom correspondence should be addressed.
E-mail: gseo@chonnam.chonnam.ac.kr

mers, the lowering of the selectivity for monomolecular skeletal isomerization with an increase in the molecular length of olefin is inevitable. However, a decrease in the activation energy for the intermediate formation of skeletal isomerization with an increase in the molecular length of 1-olefins brings about enhancement of the selectivity. The effect of molecular distribution on the preference for the monomolecular reaction, therefore, is difficult to discuss quantitatively. The fact that the selectivity dependence on molecular length of 1-olefin is different, however, according to zeolite pore structures will be a valuable piece of information for the catalytic effect of molecular distribution on zeolite catalysis.

EXPERIMENTAL

1. Preparation of Zeolite Catalysts

The FER zeolite was synthesized through a hydrothermal reaction [Seo et al., 1996], and the MFI zeolite was purchased from ZEOLYST. H-form zeolites were obtained by ion-exchange with 0.5 M ammonium nitrate (NH_4NO_3, Fluka, 99%) solution, and followed by calcination at 550 °C for 5 h. The contents of silicon and aluminum were determined by ICP (Jobin Yvon Co., JY. 38 plus). The numbers in the parentheses of FER(7.5) and MFI(25) zeolites denote their Si/Al molar ratios.

2. Characterization

BET surface areas of zeolites were calculated from nitrogen adsorption isotherms obtained at the liquid nitrogen temperature by using a home-built volumetric adsorption apparatus. Catalysts were evacuated at 300 °C for 2 h prior to nitrogen adsorption. Particle shape and size of zeolites were examined by using SEM (JEOL JSM-5400).

The acidic properties of the zeolites were investigated by the temperature-programmed desorption (TPD) of ammonia. Zeolite samples were activated in a helium flow at 550 °C for 2 h and saturated with ammonia at 80 °C through the injection of ammonia pulses. Physically adsorbed ammonia was removed by purging with a helium flow of 200 ml·min^{-1} for 2 h. Ammonia was desorbed by increasing the temperature of zeolite bed with a ramp of 10 min^{-1} and was measured by a thermal conductivity detector (TCD).

The desorption behaviors of adsorbed 1-pentene (Aldrich, 99.0%), 1-hexene (Aldrich, 97.0%) and 1-heptene (Aldrich, 97.0%) were monitored by an FT-IR spectrophotometer (BIO-RAD, FTS175C) with an *in-situ* cell made by GRASEBY SPECAC, as that of 1-butene described elsewhere [Seo et al., 2000]. A self-supported wafer of a 10 mg zeolite was evacuated under a vacuum of 0.03 Pa at 550 °C for 30 min and exposed to 30 kPa of 1-olefin vapor at 30 °C for 30 min. The catalyst was evacuated at 30 °C for 10 min to remove physically adsorbed 1-olefin. Upon heating to 550 °C under evacuation with a ramp of 16 °C·min^{-1}, IR spectra of adsorbed 1-olefin on zeolites were recorded on an absorbance mode. The scan range was 1,300-1,600 cm^{-1} and resolution 4 cm^{-1}.

3. Skeletal Isomerization of C_4-C_7 1-Olefins

The skeletal isomerization of C_4-C_7 1-olefins was performed by using an atmospheric flow reactor system described elsewhere [Seo et al., 1996]. Catalyst of 0.02-0.3 g was charged in a stainless-steel tube of 1/2" o.d. and activated in an argon flow at 550 °C for 2 h. 1-Butene (Praxair, 99.7%) was diluted with argon to have an argon/1-butene mole ratio of 2.0, and the diluted 1-butene was fed with 15 ml·min^{-1} rate. Diluted 1-pentene, 1-hexene and 1-heptene with the same molar composition of the diluted 1-butene were obtained from a bubbling argon flow through corresponding liquids in a vaporization-chamber. Partial pressure of the olefin in the feed was adjusted by controlling the temperature of the vaporization-chamber.

Gaseous products were analyzed on-line with a gas chromatograph (Varian Aerograph 1420) with a sebaconitrile column and TCD. An ice-water bath was used to collect liquid products. Liquid products were also analyzed with a gas chromatograph (Donam DS-6200) with a capillary column (HP-1, 0.2 mm×50 m) and flame ionization detector (FID). Since deactivation of the FER(7.5) and MFI(25) catalysts in skeletal isomerization of olefins was not significant, products were analyzed at the same time on stream regardless of zeolites and reaction conditions: product compositions of gas were obtained after 4 h and liquid products collected during one hour from 3 h were analyzed.

The product stream of the skeletal isomerization of 1-butene contains almost all of the hydrocarbons from C_1 to C_5, although C_4 olefins such as 2-butene and *iso*-butene are major products as well as 1-butene. Product compositions obtained from the skeletal isomerization of higher 1-olefins become more complicated. For example, the products of 1-heptene contain various C_1-C_7 hydrocarbons, especially many species of *iso*-olefins. Therefore, the conversion of 1-olefin and the selectivity for *iso*-olefins are simply defined as below, based on their mole numbers written in parentheses:

$$\text{Conversion (\%)} = \frac{(\text{1-olefin})_{feed} - (n\text{-olefins})_{effluent}}{(\text{1-olefin})_{feed}} \times 100$$

$$\text{Selectivity (\%)} = \frac{(iso\text{-olefin})_{effluent}}{(\text{1-olefin})_{feed} - (n\text{-olefins})_{effluent}} \times 100$$

Linear *n*-olefins isomerized through double bond migration from 1-olefin are not considered as products of skeletal isomerization, because the double bond migration among *n*-olefins is relatively fast compared to the skeletal isomerization. Furthermore, *n*-olefins can also be isomerized skeletally to *iso*-olefins, as well as 1-olefin.

RESULTS AND DISCUSSION

1. Characterization of Zeolite Catalysts

The particle size and Si/Al molar ratio of FER and MFI zeolites are preferred to be similar in the study of pore structure to minimize the contribution of other factors: acidity and diffusion. However, it is not usually possible to obtain zeolites with good similarities in Si/Al molar ratio and particle size, since the compositions of synthesizing gel and crystallization conditions are different according to zeolite species. Fig. 1 shows the SEM photos of the FER (7.5) and MFI(25) zeolites used in this study. The FER(7.5) zeolite is composed of large particles, particularly with a specific shape, whereas the MFI(25) zeolite is made up of small particles without any specific shape. We had tried to prepare MFI zeolites of large particles with a certain specific shape to enhance the effect of pore structure, but MFI zeolites with large and specific-shape particles were obtained only when their Si/Al molar ratios were around 100. Therefore, we used a commercially available MFI zeolite with a low Si/Al molar ratio having a sufficient amount of acid sites.

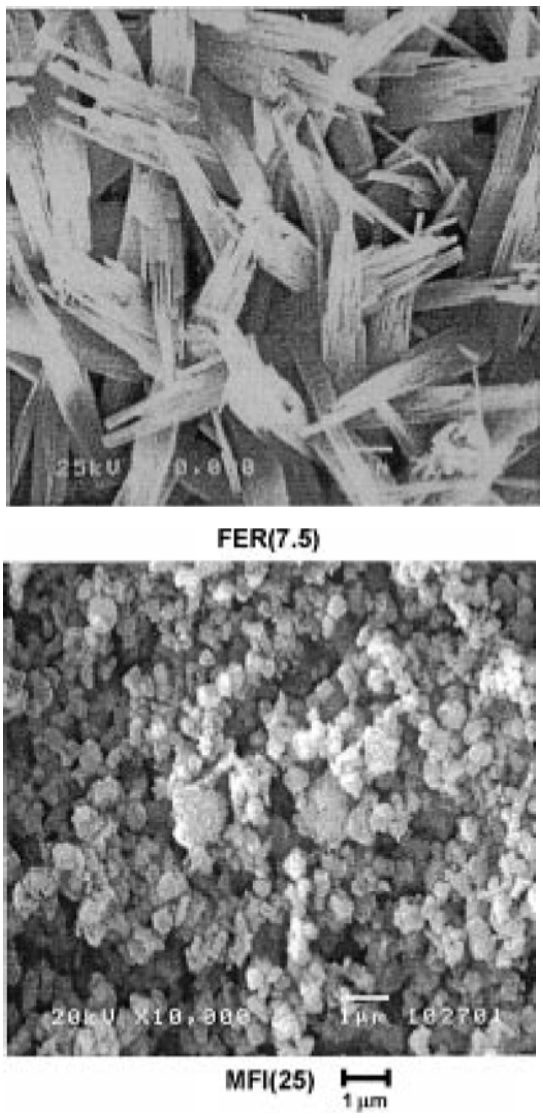

Fig. 1. SEM photos of the FER(7.5) and MFI(25) zeolites.

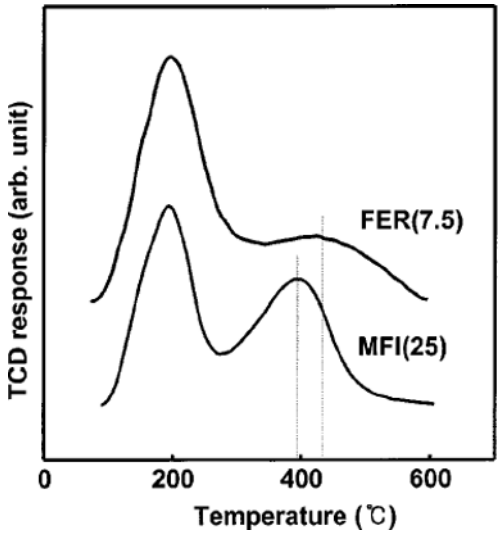

Fig. 2. TPD profiles of ammonia from the FER(7.5) and MFI(25) zeolites.

The TPD profiles of ammonia from the FER(7.5) and MFI(25) zeolites are shown in Fig. 2. Two distinct desorption peaks of ammonia were observed in both zeolites, while the peak area and the maximum temperature of the second peak were different according to zeolite species. Although there is some controversy on the first peak to be assigned as ammonia desorbed from weak acid sites [Niwa et al., 1997], the second peak is generally accepted to be attributed to ammonia desorbed from strong acid sites. The higher temperature of the second peak maximum of the FER(7.5) zeolite indicates that the FER(7.5) zeolite has stronger acid sites than the MFI(25) zeolite. On the other hand, the peak area of the second peak is considerably larger on the MFI(25) zeolite compared to the FER (7.5) zeolite, exhibiting that the number of strong acid sites is greater on the MFI(25) zeolite. It is certain that the formation of acid sites is due to the coexistence of aluminium represented by Si/Al molar ratio; however, the number of strong acid sites of zeolite measured by NH_3-TPD is largely dependent on their structures. Nevertheless, the fact that the number of strong acid sites of the FER(7.5) zeolite is small compared to that of the MFI(25) zeolite, while its acid strength is higher, is helpful for discussing their catalytic properties.

2. Skeletal Isomerization of C_4-C_7 1-Olefins

The skeletal isomerizations of C_4-C_7 1-olefins were studied on the FER(7.5) and MFI(25) zeolites with different pore structures,

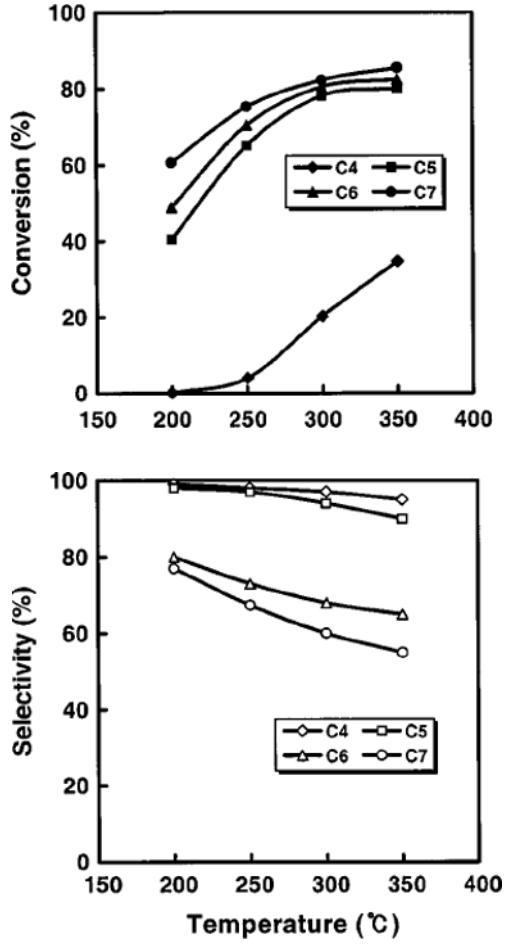

Fig. 3. Variations of the conversion and selectivity with reaction temperature in the skeletal isomerization of C_4-C_7 1-olefins over the FER(7.5) catalyst. $P_{1\text{-}olefin}$=33 kPa.

to investigate the effect of the molecular distribution in zeolite pores. Variations of the conversions and selectivities on the FER(7.5) zeolite with reaction temperature are shown in Fig. 3. Although the conversion increases with reaction temperatures for all 1-olefins, the conversion level is different. Conversions of C_5-C_7 1-olefins are high approaching 80% at 350 °C, whereas that of 1-butene is considerably lower. Low conversion of 1-butene at low temperatures may be due to its small amount of adsorbed phase and its difficulty in forming highly energetic monomolecular intermediates [Meriaudeau et al., 1997]. Besides these causes, the low content of *iso*-butene in equilibrium limits the conversion to about 30% at 350 °C. The selectivities for *iso*-olefins are high on the FER(7.5) zeolite, regardless of the molecular length of 1-olefins. And the selectivities, opposite to the conversion, decrease slightly with the reaction temperature. The selectivities for *iso*-butene and *iso*-pentenes are still high at about 90% even at 350 °C; however, those of *iso*-hexenes and *iso*-heptenes are relatively low at about 70% and 60%, respectively. Since large olefin molecules can crack without forming dimers at elevated temperatures, the selectivity for *iso*-heptene decreases with increasing temperature.

The similarity in the variations of *iso*-olefin selectivities with temperature would be expected on zeolite catalysts regardless of their molecular lengths of olefin, when the dimerization is predominant to the monomolecular skeletal isomerization. Formation of the dimer diminishes the considerable difference due to the molecular length, because even butene dimers are large enough to be cracked easily. As expected, no significant difference in the variations of conversion and selectivity with reaction temperature in the skeletal isomerization of C_4-C_7 1-olefins was observed on the MFI(25) zeolite as shown in Fig. 4. The monotonic increases in the conversion and decreases in the selectivity with the reaction temperature were similar, even though the molecular properties of C_4-C_7 1-olefins are considerably different. The concentration of activated olefin molecules should be low at a low conversion; thus, a monomolecular reaction was more preferable than a bimolecular reaction, resulting in high selectivity even on the MFI(25) zeolite. However, the increase in the concentration of activated olefin molecules in the MFI zeolite pore with increasing temperature accelerates the formation of dimers, resulting in high conversion but low selectivity due to the cracking of the dimers into various hydrocarbons.

The product distribution of 1-pentene exhibited clearly the difference in reaction paths according to zeolite species as shown in Table 1. The selectivity on the FER(7.5) zeolite was high at above 90%, but that on the MFI(25) zeolite was low at about 40%, even at similar conversion levels of around 80%. These results clearly suggest that there is a meaningful difference between the preferred reaction paths on the FER(7.5) and MFI(25) zeolites. Considerable formation of C_3 and C_4 hydrocarbons on the MFI(25) zeolite indicates that the major reaction is the dimerization followed by cracking. On the other hand, the large fraction of pentenes on the FER (7.5) zeolite indicates a negligible formation of dimers, which can be converted to various hydrocarbons.

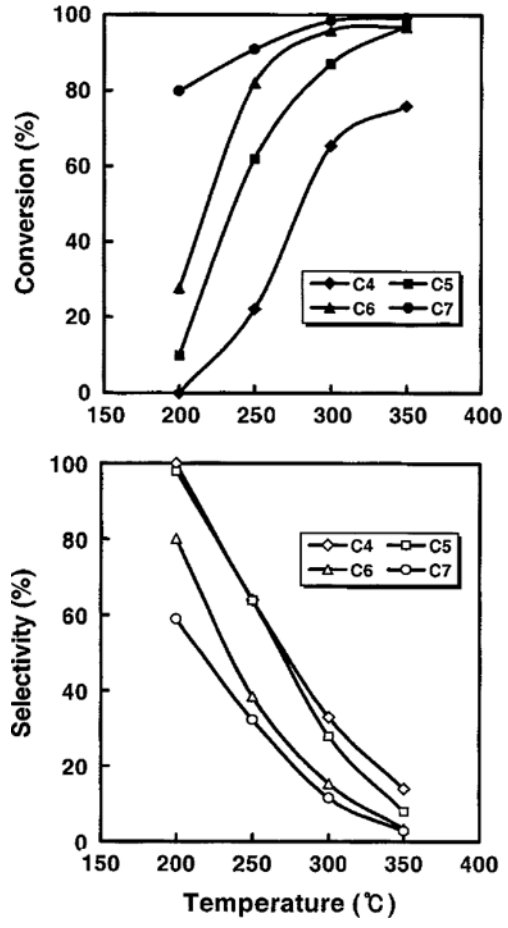

Fig. 4. Variations of the conversion and selectivity with reaction temperature in the skeletal isomerization of C_4-C_7 1-olefins over the MFI(25) catalyst. $P_{1\text{-}olefin}$=33 kPa.

Variations of the conversion and selectivity with the loading amount of catalyst also offer information about the reaction path, as well as those with the reaction temperature. Fig. 5 shows that exceptional selectivity is sustained on the FER(7.5) zeolite, even though its loading amount varies from 0.01 g to 0.3 g. The constant conversion indicates the establishment of equilibrium among pentene isomers on the FER(7.5) zeolite as does that among butene isomers [Mäurer and Kraushhaar-Czatnetzki, 1996]. The small decrease in selectivity with a large amount of catalyst loading may be due to the non-selective reaction on the external surface. On the other hand, the selectivity on the MFI(25) zeolite decreases gradually

Table 1. The skeletal isomerization of 1-pentene over the FER(7.5) and MFI(25) zeolite catalysts at 300 °C

Catalyst	Conversion (%)	Selectivity (%)	Product composition (%)						
			C_2	C_3	C_4	1-$C_5^=$	2-$C_5^=$	*iso*-$C_5^=$	C_6^+
FER(7.5)	82.1	98.1	0.1	0.7	0.6	3.1	14.8	80.5	0.2
MFI(25)	84.9	43.5	0.3	15.3	27.5	1.6	13.5	36.9	4.9

Reaction conditions - total flow rate: 15 ml·min^{-1}, catalyst loading: 0.1 g, $P_{1\text{-}pentene}$: 33 kPa.

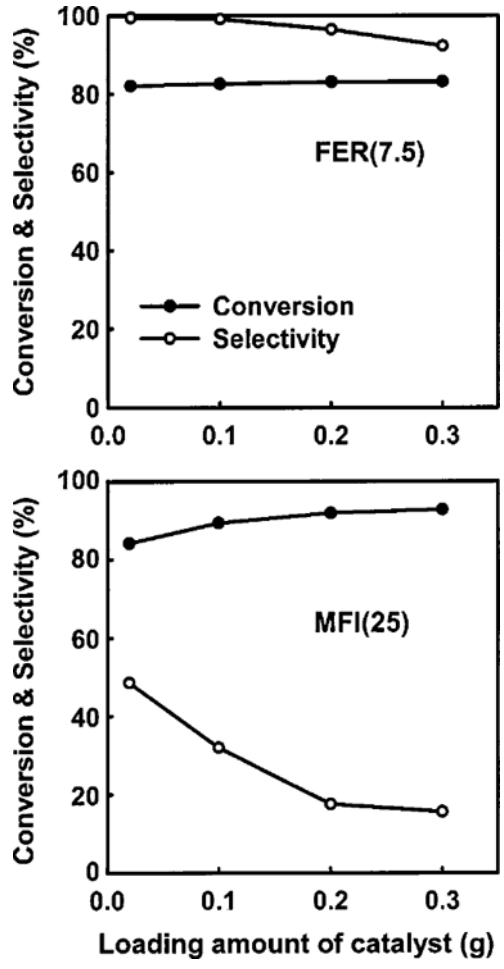

Fig. 5. Variations of the conversion and selectivity in the skeletal isomerization of 1-pentene with the loading amount of the FER(7.5) and MFI(25) catalysts at 300 °C. $P_{1\text{-}pentene}$=33 kPa.

with an increase in the catalyst loading, approaching a very low selectivity of about 20% with 0.3 g of catalyst loading.

Tremendous decreases in the selectivity with the conversion on the MFI(25) zeolite-due to the increase in the reaction temperature or loading amount-indicate that the consecutive reactions such as dimerization and cracking become predominant in MFI zeolite pore at high conversion, producing various hydrocarbons including *iso*-olefins. However, the skeletal isomerization, producing only *iso*-olefins, is selectively carried out on the FER(7.5) zeolite, sustaining the high selectivity even at high temperatures or at large amounts of catalyst loading. Furthermore, the establishment of the thermodynamic equilibrium among pentene isomers results in the constant conversion and selectivity on the FER(7.5) zeolite. These different behaviors of the FER(7.5) and MFI(25) zeolites, therefore, can be explained by the difference in the preferred reaction path: the dimerization of olefin molecules is suppressed on the FER(7.5) zeolite, while it is predominant on the MFI(25) zeolite at high conversion.

3. Molecular Distribution of C_4-C_7 *iso*-olefins in the Zeolite Pore

Distribution patterns of 1-olefin molecules in zeolite pores work as a determining factor for the preference of olefin molecules to the reaction path: monomolecular skeletal isomerization or bimolecular dimerization followed by cracking. The probable distribution of 1-olefin molecules in zeolite pores was simulated by using Cerius^2 Sorption Module of Molecular Simulation at 25 °C and under 100 kPa as described elsewhere [Seo et al., 1997]. Fig. 6 sketches the simulated molecular distribution of 1-olefins in the pores of FER and MFI zeolites. Molecules and pores are drawn with the same scale. Shadowed molecules mean the absence of adsorbed molecules. 1-Butene molecules are nicely confined in the cages of FER zeolite pores, while 1-petene, 1-hexene and 1-heptene molecules are too large to be completely confined. It is possible for 1-butene molecules to be distributed in each cavity, but the reduction of simulated adsorbed amount of 1-pentene suggests that only a half of the cavity is occupied by adsorbed molecules. Although molecular lengths of C_5-C_7 olefin exceed the cavity size, a close distribution such as one molecule per cavity is not allowed due to restriction of pore structure and repulsion between adsorbed olefin

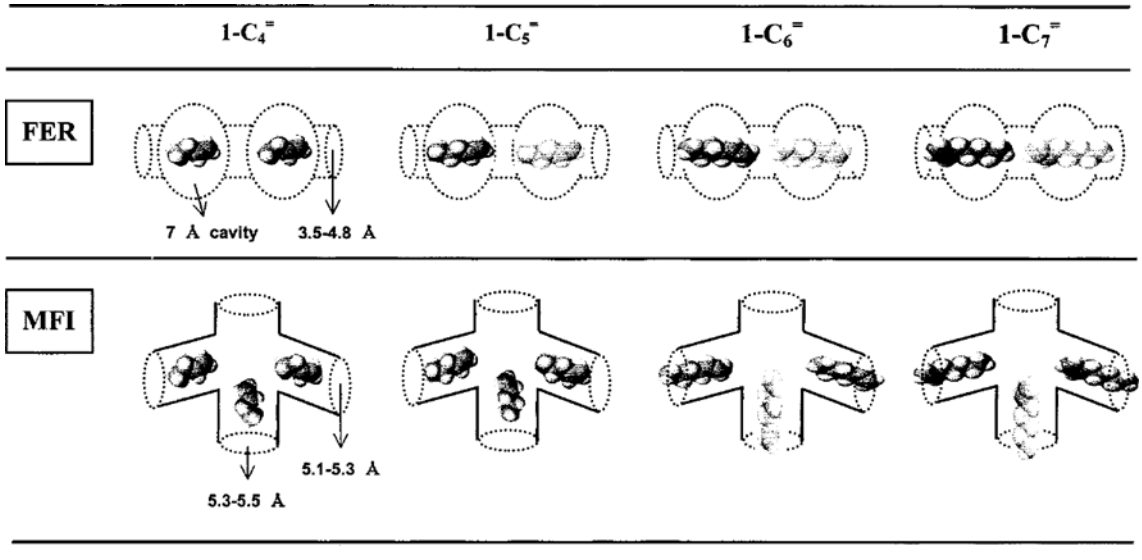

Fig. 6. Schematic drawing for the distribution of 1-olefin molecules in FER and MFI zeolite pores.

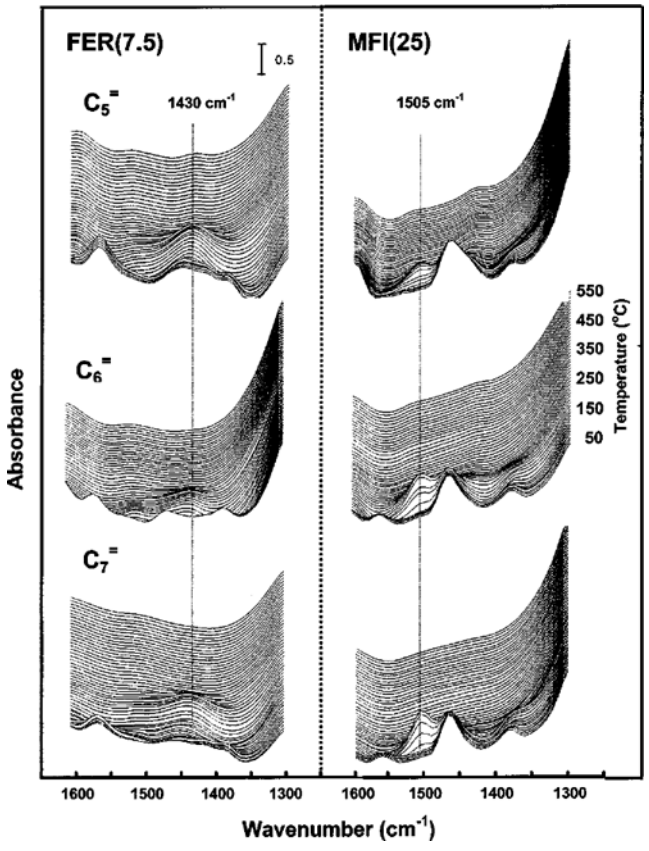

Fig. 7. 3-D IR spectra of adsorbed 1-pentene, 1-hexene and 1-heptene on the FER(7.5) and MFI(25) zeolites. Zeolite was exposed to 1-olefins at 30 °C and IR spectra were recorded with increasing evacuation temperature to 550 °C.

molecules. Thus, the confinement of 1-butene molecules in the cavity and sparse distribution of C_5-C_7 olefin suppress the dimerization, expecting the high selectivity for the skeletal isomerization.

Otherwise, there is no remarkable difference in the molecular distribution of C_4-C_7 1-olefins in the MFI zeolite pore, even though the molecular size of 1-olefins varies from 1-butene to 1-heptene. The large cross-sectional area does not impose on the 1-olefin molecules a specific distribution pattern.

The difference in the molecular distribution of 1-olefins in FER and MFI zeolites induces different behaviors of adsorption-desorption. Fig. 7 shows the 3-D IR spectra of adsorbed 1-pentene, 1-hexene and 1-heptene on the FER(7.5) and MFI(25) zeolites recorded by increasing the evacuation temperature. These IR spectra of adsorbed olefins are similar to those of adsorbed 1-butene reported in our previous paper [Seo et al., 2000], except the complete desorption of 1-butene from the FER(7.5) zeolite with evacuation even at ambient temperature. The higher boiling temperatures of C_5-C_7 1-olefins compared to 1-butene require higher evacuation temperature for their complete desorption from the FER zeolite.

Absorption bands of 1,430 cm^{-1} assigned to the adsorbed olefin were observed by adsorption of C_5-C_7 1-olefins on the FER(7.5) zeolite, and retained at about 200 °C. However, the band disappeared by further increasing the evacuation temperature without any change indicating chemical reactions.

Absorption bands of 1-olefin on the MFI(25) zeolite were stronger than those on the FER(7.5) zeolite. At ambient temperature a strong absorption band at 1,470 cm^{-1} was consistently observed from C_5-C_7 1-olefins adsorbed on the MFI(25) zeolite. Furthermore, the temperature increase induced the appearance of a new absorption band at 1,505 cm^{-1} accompanied by the diminishment at the 1,470 cm^{-1} band. The absorption band at 1,505 cm^{-1} is assigned to polymeric species formed from olefin on zeolite surface [Trombetta et al., 1997]. Therefore, the appearance of this absorption band demonstrates the dimer formation from olefins on the MFI(25) zeolite, because polymeric species are consecutive products of olefin dimerization. The same IR spectra of adsorbed 1-olefins such as 1-pentene, 1-hexene and 1-heptene, indicate the same distribution patterns of adsorbed olefin molecules in the MFI zeolite.

The retention of 1-olefin on the MFI(25) zeolite is not attributed to the strong interaction between adsorbed olefin molecules and acid sites, because the acid strength of the MFI(25) zeolite is considerably weaker than that of the FER(7.5) zeolite. Since *n*-heptane molecules are desorbed easily from both FER(7.5) and MFI(25) zeolites with evacuation at ambient temperature [Seo et al., 2000], the retention of 1-olefin is not related to the molecular weight. Therefore, the retention of olefin molecules and conversion to polymeric species on the MFI(25) zeolite demonstrate the formation of dimers or oligomers in pores even at ambient temperature. Otherwise, monomolecularly distributed 1-olefin molecules in the FER(7.5) zeolite pore are desorbed without further conversion to other species. Different pore structures of zeolites cause the differences in molecular distributions of olefins and in further reactions among adsorbed olefinic species.

CONCLUSIONS

Skeletal isomerization of C_4-C_7 1-olefins on zeolite catalysts is largely dependent on their pore shapes: however, the difference in the molecular distribution due to their molecular length also influences the selectivity. Although the FER(7.5) zeolite exhibits a high selectivity for C_4-C_7 *iso*-olefins compared to the MFI(25) zeolite, the selectivities for *iso*-hexenes and *iso*-heptenes are considerably lower than those for *iso*-butene and *iso*-pentene. Besides the monomolecular cracking of large olefin without forming dimers, the incomplete confinement of large molecules in cavities lowers the monomolecular reaction selectivity. On the other hand, the MFI(25) zeolite shows no significant difference in the selectivity with change in the molecular length of 1-olefins: the selectivity decreases drastically by increasing the conversion for C_4-C_7 olefins. Negligible restriction of the molecular distribution of olefin on the MFI(25) zeolite does not suppress dimerization, resulting in the low selectivity. Therefore, the molecular distribution of 1-olefin in zeolite pores is an important factor in determining the preference for monomolecular skeletal isomerization, when the monomolecular cracking of olefin is not predominant.

ACKNOWLEDGEMENT

This research was supported by the Korea Science and Engineering Foundation (971-1108-052-2). The authors would like to thank Korea Basic Science Institute/GwangJu Branch for the help in ICP measurement.

REFERENCES

Asensi, M. A. and Martinez, A., "Selective Isomerization of *n*-Butenes to Isobutene on High Si/Al Ratio Ferrierite in the Absence of Coke Deposits: Implications on the Reaction Mechanism," *Appl. Catal. A: General*, **183**, 155 (1999).

Butler, A. C. and Nicolaides, C. P., "Catalytic Skeletal Isomerization of Linear Butenes to Isobutene," *Catal. Today*, **18**, 443 (1993).

Choudhary, V. R., "Catalytic Isomerization of *n*-Butene to Isobutene," *Chem. Ind. Dev.*, **8**, 32 (1974).

Jousse, F., Leherte, L. and Vercauteren, D. P., "Molecular Mechanical Investigation of the Energetics of Butene Sorbed in H-Ferrierite," *J. Mol. Simulation*, **17**, 175 (1996).

Jousse, F., Leherte, L. and Vercauteren, D. P., "Energetics and Diffusion of Butene Isomers in Channel Zeolites from Molecular Dynamics Simulations," *J. Mol. Catal. A: Chemical*, **119**, 165 (1997).

Kim, N.-H., Kim, J.-H. and Seo, G., "Skeletal Isomerization of 1-Butene over Alkali-Modified Silica-Alumina Catalysts," *HWAHAK KONGHAK*, **36**, 571 (1998).

Kim, W.-G., Kim, N.-H., Kim, J.-H. and Seo, G., "High Selectivite Skeletal Isomerization of 1-Butene over Phosphorus-Modified Silica-Alumina," *Korean J. Chem. Eng.*, **16**, 392 (1999).

Lee, H. C., Woo, H. C., Ryoo, R., Lee, K. H. and Lee, J. S., "Skeletal Isomerization of *n*-Butenes to Isobutene over Acid-treated Natural Clinoptilolite Zeolites," *Appl. Catal. A: General*, **196**, 135 (2000).

Mäurer, T. and Kraushhaar-Czatnetzki, B., "Thermodynamic and Kinetic Reaction Regimes in the Isomerization of 1-Pentene over ZSM-5 Catalysts," *J. Catal.*, **187**, 202 (1999).

Meriaudeau, P., Tuan, V. A., Le, L. H. and Szabo, G., "Selective Isomerization of *n*-Butene into Isobutene over Deactivated H-Ferrierite Catalyst: Further Investigations," *J. Catal.*, **169**, 397 (1997).

Niwa, M. and Katada, N., "Measurements of Acidic Property of Zeolites by Temperature Programmed Desorption of Ammonia," *Catal. Surv. from Japan*, **1**, 215 (1997).

Seo, G., Jeong, H. S., Hong, S. B. and Uh, Y. S., "Skeletal Isomerization of 1-Butene over Ferrierite and ZSM-5 Zeolites: Influence of Zeolite Acidity," *Catal. Lett.*, **36**, 249 (1996).

Seo, G., Jeong, H. S., Lee, J.-M. and Ahn, B. J., "Seletivity to the Skeletal Isomerization of 1-Butene over Ferrierite (FER) and ZSM-5 (MFI) Zeolites," *Stud. Surf. Sci. Catal.*, **105**, 1431 (1997).

Seo, G., Kim, N.-H., Lee, Y.-H. and Kim, J.-H., "Skeletal Isomerization of 1-Butene over Mesoporous Materials," *Catal. Lett.*, **57**, 209 (1999).

Seo, G., Kim, M.-Y. and Kim, J.-H., "IR Study on the Reaction Path of Skeletal Isomerization of 1-Butene," *Catal. Lett.*, **67**, 207 (2000).

Trombetta, M., Busca, G., Rossin, S., Piccoli, V. and Cornaro, U., "FT-IR Studies on Light Olefin Skeletal Isomerization Catalysis," *J. Catal.*, **168**, 349 (1997).

van Well, W. J. M., Cottin, X., de Haan, J. W., Smit, B., Nivarthy, G., Lercher, J. A., van Hooff, J. H. C. and van Santen, R. A., "Chain Length Effects of Linear Alkanes in Zeolite Ferrierite. 1. Sorption and ^{13}C NMR Experiments," *J. Phys. Chem. B*, **102**, 3945 (1998).